



# Fluorescent probe partitioning in GUVs of binary phospholipid mixtures: Implications for interpreting phase behavior

Janos Juhasz<sup>a,b,1</sup>, James H. Davis<sup>a,b</sup>, Frances J. Sharom<sup>b,c,\*</sup>

<sup>a</sup> Department of Physics, University of Guelph, Guelph, ON, Canada N1G 2W1

<sup>b</sup> Biophysics Interdepartmental Group, University of Guelph, Guelph, ON, Canada N1G 2W1

<sup>c</sup> Department of Molecular and Cellular Biology, University of Guelph, Guelph, ON, Canada N1G 2W1

## ARTICLE INFO

### Article history:

Received 30 May 2011

Received in revised form 25 August 2011

Accepted 8 September 2011

Available online 16 September 2011

### Keywords:

Phase transition

Giant unilamellar vesicle

Fluorescent probe

Confocal fluorescence microscopy

Partitioning

Patch and fibril domains

## ABSTRACT

The phase behavior of membrane lipids is known to influence the organization and function of many integral proteins. Giant unilamellar vesicles (GUVs) provide a very useful model system in which to examine the details of lipid phase separation using fluorescence imaging. The visualization of domains in GUVs of binary and ternary lipid mixtures requires fluorescent probes with partitioning preference for one of the phases present. To avoid possible pitfalls when interpreting the phase behavior of these lipid mixtures, sufficiently thorough characterization of the fluorescent probes used in these studies is needed. It is now evident that fluorescent probes display different partitioning preferences between lipid phases, depending on the specific lipid host system. Here, we demonstrate the benefit of using a panel of fluorescent probes and confocal fluorescence microscopy to examine phase separation in GUVs of binary mixtures of 1,2-dioleoyl-*sn*-glycero-3-phosphocholine (DOPC)/1,2-dipalmitoyl-*sn*-glycero-3-phosphocholine (DPPC). Patch and fibril gel phase domains were found to co-exist with liquid disordered ( $l_d$ ) domains on the surface of GUVs composed of 40:60 mol% DOPC/DPPC, over a wide range of temperatures (14–25 °C). The fluorescent lipid, 1,2-dipalmitoyl-*sn*-glycero-3-phosphoethanolamine-N-(7-nitro-2-1,3-benzoxadiazol-4-yl) (NBD-DPPE), proved to be the most effective probe for visualization of fibril domains. In the presence of Lissamine<sup>TM</sup> rhodamine B 1,2-dihexadecanoyl-*sn*-glycero-3-phosphoethanolamine (Rh-DPPE) we were unable to detect fibril domains. This fluorophore also affected the partitioning behavior of other fluorescent probes. Overall, we show that the selection of different fluorescent probes as lipid phase reporters can result in very different interpretation of the phase behavior of DOPC/DPPC mixtures.

© 2011 Elsevier B.V. All rights reserved.

## 1. Introduction

The organization, behavior and function of integral proteins in cellular membranes are believed to be regulated by the phase behavior of the surrounding lipid bilayer. For more than 30 years, binary mixtures

and, more recently, ternary mixtures of lipids have served as models for biomembranes, and intensive research has focused on elucidating phase equilibria in these lipid mixtures. Results emerging from model membrane studies have led to important new concepts in the field of biomembranes, such as the “lipid raft” hypothesis [1–3]. A relatively novel model membrane system, giant unilamellar vesicles (GUVs), allows the examination of physical processes such as lipid phase separation at the microscopic level using fluorescence imaging. Thus, the different physical forms of lipid phases can be visualized directly by the use of fluorescent probes with known phase partitioning preference. However, a thorough examination of the behavior of these probes is essential in drawing firm conclusions about the phase state of a membrane system, especially since it is now apparent that the phase preference of a fluorescent probe depends on the local physicochemical environment within the lipid domains [4]. Reports of fluorescent probe partitioning inconsistencies are increasing, and fluorescent probes have been found to display different partitioning preference in different lipid systems, or even in the same lipid system when used with other fluorescent probes in dual or triple labeling approaches [5]. Sample preparation differences may also lead to the observation of very different phase behavior in the same lipid system.

**Abbreviations:** Bodipy-PC, 2-(4,4-difluoro-5,7-dimethyl-4-bora-3a,4a-diaza-s-indacene-3-pentanoyl)-1-hexadecanoyl-*sn*-glycero-3-phosphocholine; CFM, confocal fluorescence microscopy; DiD, 1,1'-dioctadecyl-3,3',3'-tetramethylindodicarbocyanine 4-chlorobenzenesulfonate salt; DiC<sub>18</sub>, 1,1'-dioctadecyl-3,3',3'-tetramethylindodicarbocyanine perchlorate; DLPC, 1,2-dilauroyl-*sn*-glycero-3-phosphocholine; DOPC, 1,2-dioleoyl-*sn*-glycero-3-phosphocholine; DPPC, 1,2-dipalmitoyl-*sn*-glycero-3-phosphocholine; GUV, giant unilamellar vesicle; ITO, indium tin oxide; MLVs, multilamellar vesicles; NBD-DPPE, 1,2-dipalmitoyl-*sn*-glycero-3-phosphoethanolamine-N-(7-nitro-2-1,3-benzoxadiazol-4-yl); NMR, nuclear resonance spectroscopy; POPC, 1-palmitoyl-2-oleoyl-*sn*-glycerophosphocholine; Rh-DPPE, Lissamine<sup>TM</sup> rhodamine B 1,2-dihexadecanoyl-*sn*-glycero-3-phosphoethanolamine; TR-DPPE, Texas Red 1,2-dihexadecanoyl-*sn*-glycero-3-phosphoethanolamine

\* Corresponding author at: Department of Molecular and Cellular Biology, University of Guelph, Guelph, ON, Canada N1G 2W1. Tel.: +1 519 824 4120x52247; fax: +1 519 837 1802.

E-mail address: [fsharom@uoguelph.ca](mailto:fsharom@uoguelph.ca) (F.J. Sharom).

<sup>1</sup> Present address: Department of Medical Physics, Juravinski Cancer Centre at Hamilton Health Sciences, Hamilton, ON, Canada L8V 5C2.

We recently characterized the behavior of a panel of commonly used fluorescent probes in GUVs of “lipid raft” mixtures containing 1,2-dioleoyl-*sn*-glycero-3-phosphocholine (DOPC), 1,2-dipalmitoyl-*sn*-glycero-3-phosphocholine (DPPC), and cholesterol [5]. Here we present results from single, dual and triple labeling experiments in GUVs of a binary mixture of DOPC/DPPC. Our goals were to characterize the partitioning behavior of a panel of fluorescent probes in co-existing liquid disordered ( $l_d$ ) and gel phases, and examine the phase behavior of this lipid mixture in more detail. Li and Cheng previously reported the presence of two novel gel phases in GUVs of DOPC/DPPC mixtures using confocal fluorescence microscopy (CFM) [6]. Patch and fibril (stripe) domains were observed on the surface of the GUVs, depending on the mole fraction of DPPC and the temperature. Because fibril domains appear to be present only at higher DPPC mole fractions at room temperature, we examined the partitioning preference of the panel of fluorescent probes in 40:60 mol% DOPC/DPPC. The present study represents the first time that the behavior of several of these probes (e.g. NBD-DPPE) has been characterized in this binary lipid mixture. Novel approaches were employed using single, dual (pairs of probes), and triple (three probes used simultaneously) fluorescence labeling. We report that the presence of one particular probe makes it impossible to detect fibril domains, not only when used by itself, but also when combined with other probes in dual and triple labeling experiments. We believe that bringing to light these important effects of fluorescent probes on phase separation in binary lipid mixtures will serve as a guide in interpreting the phase behavior of more complex membrane systems.

## 2. Materials and methods

### 2.1. Materials

DOPC, DPPC, and DPPC- $d_{62}$  were obtained from Avanti Polar Lipids (Alabaster, AL). Texas Red 1,2-dihexadecanoyl-*sn*-glycero-3-phosphoethanolamine (TR-DPPE), 1,1'-dioctadecyl-3,3,3',3'-tetramethylindocarbocyanine perchlorate (DiIC<sub>18</sub>), 1,1'-dioctadecyl-3,3,3',3'-tetramethylindocarbocyanine 4-chlorobenzenesulfonate salt (DiD), Lissamine<sup>TM</sup> rhodamine B 1,2-dihexadecanoyl-*sn*-glycero-3-phosphoethanolamine (Rh-DPPE), and 2-(4,4-difluoro-5,7-dimethyl-4-bora-3a,4a-diaza-*s*-indacene-3-pentanoyl)-1-hexadecanoyl-*sn*-glycero-3-phosphocholine (Bodipy-PC) were all from Invitrogen, while 1,2-dipalmitoyl-*sn*-glycero-3-phosphoethanolamine-N-(7-nitro-2-*l*,3-benzoxadiazol-4-yl) (NBD-DPPE) was supplied by Avanti Polar Lipids. The molecular structures of these fluorescent lipid probes are shown in Supplementary Fig. S1.

### 2.2. Sample preparation

GUVs were prepared by electroformation on a pair of platinum (Pt) wires by a method first developed by Angelova and Dimitrov [7,8], modified as previously described [5,9]. Lipid stock solutions were prepared in chloroform/methanol 2:1 (v/v) at a concentration of 0.27 mg/mL, and appropriate volumes of each were mixed. Labeling was carried out by pre-mixing the desired fluorescent probes with the lipids in organic solvent. The concentration of individual fluorescent probes in each sample was  $0.1 \pm 0.01$  mol%, except for the triple labeling experiment with Bodipy-PC/Rh-DPPE/DiD, where the concentration of each probe in the sample was  $0.05 \pm 0.01$  mol%. Drops of  $\sim 2 \mu\text{L}$  of lipids and fluorescent labels in organic solvent were deposited on Pt wires under a stream of N<sub>2</sub> gas. The Pt wires were placed in a vacuum for  $\sim 1$  h to completely remove the organic solvent. One side of the chamber was then sealed with a coverslip using a small amount of silicone grease. Heated ( $\sim 60$  °C) high purity water (Millipore SuperQ) was added to the chamber until it covered the Pt wires, and then the other side of the chamber was sealed with another coverslip. The chamber was placed in an oven (Isotemp

500 series, Fisher Scientific, Mississauga, ON, Canada), and the Pt wires were connected to a function generator (HP 3310A or BK Precision 4011A). A sinusoidal wave function of amplitude 3 V and frequency 10 Hz was applied for about 90 min, after which the electric field was turned off and the chamber was placed on the microscope stage. Typically an equilibration time of at least 10 min was allowed before proceeding with the temperature scans, which usually started at 42 °C and involved progressive cooling to lower temperatures. Because we observed different phase behavior than Li and Cheng [6] when using Rh-DPPE as one of the fluorescent probes, we highlight below the sample preparation differences. Li and Cheng employed indium tin oxide (ITO) coated glass slides for electroformation instead of Pt wires, and the Rh-DPPE label was used at 0.4 mol%. The same frequency for the sinusoidal wave function, and comparable voltages, were used as the present study. They employed a temperature during electroformation of 50 °C and a sample cooling rate of 0.13 °C/min. We used sample cooling rates in the range 0.2–2.0 °C/min.

### 2.3. Confocal fluorescence microscopy

A custom-made imaging chamber described previously [5,9] was employed for imaging the GUVs by CFM. The sample temperature was controlled ( $\pm 0.1$  °C) above room temperature by applying an electric current to the imaging chamber (TC-324B, Warner Instruments, Hamden, CT) and below room temperature by circulating water from a temperature-controlled bath (Isotemp 3016, Fisher Scientific) underneath the sample compartment. Two thermistors were used to monitor the temperature, one connected to the imaging chamber and the other placed in the sample compartment (cable assembly for series 20 chambers, CC-28, Warner Instruments). The temperature values stated in the text are the readings from the thermistor situated in the sample compartment between the two Pt wires, which were separated by 3 mm. The cooling rate from a set-point temperature was 1–2 °C per min; this rate slowed as the temperature approached the new set-point temperature. Occasionally, the temperature controller was turned off and the sample was allowed to equilibrate to room temperature at an average cooling rate of 0.2–0.5 °C/min. Typically, different sections of the Pt wires were checked for consistency of the onset of the phase co-existence and detection of the different patch and fibril domains. The onset of  $l_d$ -gel phase co-existence were determined from observations of at least 50 separate GUVs generated from at least two different lipid droplets on the Pt wires, by lowering the temperature through the miscibility transition temperature. Images were acquired on commercial Leica confocal microscopes (Leica, Heidelberg, Germany), either on a CLSM-U (an upright Leica DM RE microscope connected to a Leica TCS SP2 system), or on a CLSM-MP (an upright Leica DM 6000B microscope connected to a Leica TCS SP5). The following objectives were used to image the samples: a 20 $\times$  air objective (not touching the sample) with numerical aperture (NA) of 0.5, a 40 $\times$  water immersion objective of NA 0.8, and a 60 $\times$  water immersion objective of NA 0.9. The excitation wavelength used for NBD-DPPE and Bodipy-PC was 488 nm, while 543 nm was used for TR-DPPE, DiIC<sub>18</sub>, and Rh-DPPE. DiD was excited at 633 nm. The confocal pinhole settings were in the range 1–2 Airy, 1 Airy being the default value used for a given objective. The intensity of the lasers was kept at  $\sim 60\%$ . All images were routinely checked for under- and over-exposure using the Qlut function in the Leica confocal software. We typically used 1024 pixel  $\times$  1024 pixel resolution with a 400 Hz or 800 Hz scan speed, and a line average of typically 2 or 4, but occasionally 8. When using combinations of fluorescent probes in CFM, care was taken to rule out artifacts relating to “bleed-through” of one probe's fluorescence emission signal in the detection channel of another probe. This was necessary when using NBD-DPPE together with DiIC<sub>18</sub>, because of the large overlap of their emission signals. Typically, the excitation and/or detection in one channel were turned off, and the acquired image in the other channel was compared with the image acquired with both channels active.

### 3. Results and discussion

#### 3.1. Visualization of the gel-liquid disordered phase transition in GUVs by CFM

Our goal was to first compare the onset temperature of the  $l_d$ -gel phase transition observed in mixtures of DOPC/DPPC using CFM with the values obtained by deuterium nuclear resonance ( $^2\text{H}$  NMR) spectroscopy, and then characterize the partitioning preference of the various fluorescent lipid probes. The direct visualization of the onset of the  $l_d$ -gel phase co-existence in GUVs of binary mixtures of DOPC/DPPC is somewhat different from that of the  $l_d$ - $l_o$  phase co-existence in ternary mixtures of DOPC/DPPC/cholesterol [5]. Domain equilibration takes place at a much slower rate in binary compared to ternary mixtures. We attribute this to the reduced molecular motions in the gel phase. Therefore, accurate detection of the onset of phase separation requires a longer waiting time after setting the new temperature. Similarly, reversing the phase separation took somewhat longer in binary mixtures than in ternary mixtures. In addition, as observed in our earlier studies on ternary mixtures of GUVs, not all the GUVs in the field of view phase-separated at the same temperature. The temperature range in which all GUVs (both in the field of view and in other regions on the Pt wires) phase-separated was  $\sim 4^\circ\text{C}$  at most, as opposed to a range of  $\sim 1^\circ\text{C}$  recorded for ternary mixtures.

To determine the  $l_d$ -gel phase miscibility temperature we used TR-DPPE as the phase transition reporter, since it had proved to be a reliable fluorescent probe in ternary mixtures [5,9]. To examine the phase transition temperature, we prepared three different concentrations of DOPC/DPPC: 70:30, 60:40, and 40:60 mol%. We specifically monitored the onset of the  $l_d$ -gel phase separation, and in agreement with earlier studies, TR-DPPE was found to partition into the  $l_d$  phase in GUVs of DOPC/DPPC [10]. The recorded temperature values of the onset of the  $l_d$ -gel phase co-existence were higher than expected, based on the recently published phase diagram for this lipid system [11]; they were  $32^\circ\text{C}$ ,  $36^\circ\text{C}$ , and  $38^\circ\text{C}$  for DOPC/DPPC mixtures of 70:30, 60:40, and 40:60 mol%, respectively. All GUVs in the imaging chamber (typically, 70–100 GUVs were examined) phase-separated at the temperature stated above  $\pm 2^\circ\text{C}$  at most. These temperature values are 4–8  $^\circ\text{C}$  higher than expected from  $^2\text{H}$  NMR measurements on multilamellar vesicles (MLVs) [11], considering the fact that undeuterated samples are expected to phase-separate  $\sim 3.5^\circ\text{C}$  higher at most, depending on the DOPC:DPPC ratio. The higher the amount of DPPC in GUVs, the more significant was the observed effect of perdeuteration on the phase boundaries when undeuterated and deuterated samples were compared.

Using GUVs of DOPC/DPPC, other groups have measured higher transition temperatures than those suggested by the proposed phase diagrams for this lipid mixture. In particular, Beattie et al. [12] reported a phase transition temperature  $\sim 8^\circ\text{C}$  higher than expected from the phase diagrams [11,13], when using 0.8 mol% TR-DPPE as the reporter probe. Using supported bilayers of DOPC/DPPC and 0.5 mol% DiI $_{18}$ , Bernchou and co-workers [14] measured a transition temperature  $\sim 3^\circ\text{C}$  higher when compared to the temperature value suggested by the phase diagram [11,13]. When Bouvrais et al. used Rh-DPPE at 0.5 and 2 mol% in GUVs of 1-palmitoyl-2-oleoyl-*sn*-glycerophosphocholine (POPC), and either an epifluorescence or phase contrast imaging system, they found that GUVs exposed to light exhibited facets, whereas GUVs protected from light did not [15]. They attributed this effect to possible peroxide formation arising from photo-oxidation effects, rather than to electroformation of GUVs on Pt wires. It should be noted that we did not observe any spontaneous facet formation in our samples. Morales-Pennington et al. attributed the phase boundary shift towards higher temperatures in DOPC/18:0-sphingomyelin/cholesterol mixtures to lipid oxidation effects [16]. In the present study, great care was taken to minimize possible oxidation effects, and we believe that oxidation effects play a minor role in the transition temperature increase in our samples, if at all.

For a more direct comparison with the  $^2\text{H}$  NMR data, we prepared GUVs of 40:60 mol% DOPC/DPPC- $d_{62}$  labeled with TR-DPPE. Confocal fluorescence images of the phase transition in these GUVs are presented in Fig. 1. No change in fluorescence intensity was observed in the  $42.3$ – $34^\circ\text{C}$  temperature range (Fig. 1A and B). Small dark spots, or quasi-circular patch domains, corresponding to the gel phase were detectable starting at  $\sim 32.3^\circ\text{C}$  (Fig. 1C), particularly in larger GUVs. On increasing the temperature to  $33.6^\circ\text{C}$  and equilibrating the sample at this temperature for  $\sim 5$  min, patch domains completely vanished from the surface of the GUVs. When the temperature was lowered to  $31^\circ\text{C}$  once more, patch domains became visible again at  $32.1^\circ\text{C}$  (not shown), demonstrating the reversibility of their formation. At  $31^\circ\text{C}$  the proportion of patch domains increased, and additional smaller patch domains appeared on the surface of the GUVs (Fig. 1D). The domains moved across the surface of the GUVs considerably more slowly than the  $l_o$  domains observed in GUVs of ternary lipid mixtures [5,9]. We observed patch domains at contact areas between GUVs, where they remained during the duration of the experiment (arrows in Fig. 1D). Some GUVs underwent phase separation such that one small patch domain appeared first at the contact region and then remained stationary, so that only the domain size increased as the temperature decreased. We also observed this effect in GUVs labeled with other fluorescent probes. This so-called “pinning” of solid domains in GUVs has previously been reported for other binary lipid mixtures [17].

After lowering the set temperature further, an image was acquired at  $27.2^\circ\text{C}$  before the temperature reached the equilibrium value (shown in Fig. 1E). The edges of the patch domains were clearly seen to begin dispersing into short fibrils, and TR-DPPE started to partition

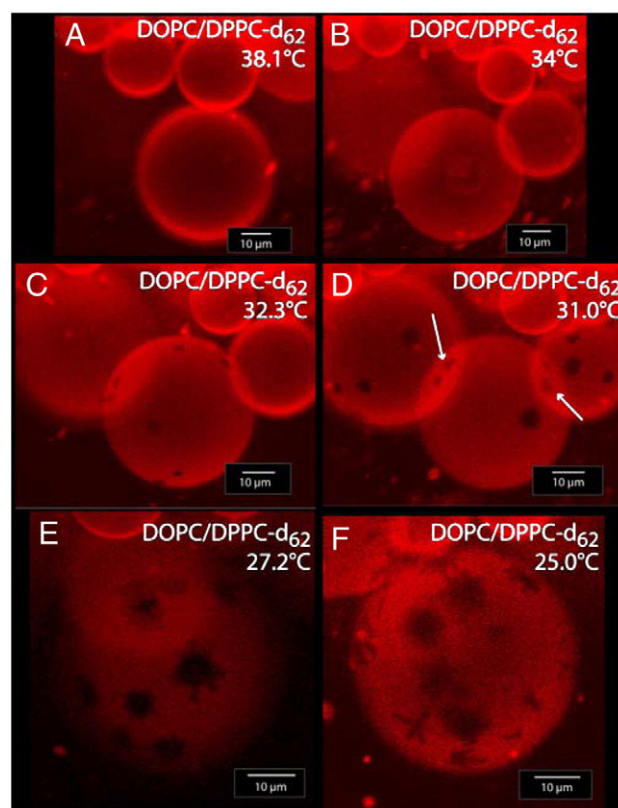


**Fig. 1.** Phase separation in GUVs of DOPC/DPPC- $d_{62}$ . CFM images of 40:60 mol% DOPC/DPPC- $d_{62}$  GUVs labeled with TR-DPPE. Homogeneous  $l_d$  phase is detected in (A) at  $38.1^\circ\text{C}$  and (B) at  $34^\circ\text{C}$ .  $l_d$ -gel phase co-existence starts in (C) at  $32.3^\circ\text{C}$  when patch domains become visible on the surface of the GUVs. The proportion of gel phase increases at  $31^\circ\text{C}$  in (D). The emergence of fibril domains from patch domains is detected starting at  $27.2^\circ\text{C}$  in (E). Evidence for the expansion of fibril domains over the surface of a GUV is seen at  $25^\circ\text{C}$  in (F). The arrows in (D) indicate stationary patch domains located at the contact regions between GUVs.



away from these fibril domains. After equilibrating the sample at 27.1 °C, the fibril domains began to extend over the vesicle surface (not shown). The image in Fig. 1F at 25 °C was acquired after an equilibration time of more than 10 min, and clearly shows that, on cooling, the fibril domains had extended even further over the GUV surface. However, the fibril domains did not form an interconnected network on the surface of vesicles maintained at room temperature (22 °C). We did not explore lower temperature ranges for this sample.

The onset of the  $l_d$ -gel phase co-existence for this lipid mixture was between 33.0 and 30.5 °C. All GUVs in the sample phase-separated (i.e. the presence of patch domains could be confirmed) within a temperature range of ~2.5 °C. We routinely checked GUVs in different regions of the Pt wires, and the phase separation was consistent for all. These values are in agreement with the recently published DOPC/DPPE- $d_{62}$  phase diagram [11], which indicates that this sample enters the  $l_d$ -gel two phase co-existence region at ~30 °C on cooling. However, inspection of the  $^2\text{H}$  NMR spectra suggests an upper limit for phase boundaries of 30–32 °C at 40:60 mol% composition. A better method for comparing results from the CFM and  $^2\text{H}$  NMR techniques would be to measure gel domain area fractions in GUVs, and compare them to the proportions of gel phase calculated from the  $^2\text{H}$  NMR phase diagram in a similar manner as presented for GUVs exhibiting  $l_d$ - $l_o$  phase co-existence [9]. However, it is challenging to estimate gel domain area fractions from CFM images of GUVs, since the domains are not circular. Nevertheless, Fidorra et al. recently presented a feasible way to assess fibril-like gel phase area fractions in binary mixtures of phospholipids [18]. Because our major focus was on the partitioning preference of commonly used fluorescent probes, we have not attempted to resolve the observed differences in miscibility temperature of DOPC/DPPE and DOPC/DPPE- $d_{62}$  mixtures.

According to Li and Cheng [6], fibril domains in GUVs of DOPC/DPPE mixtures are in the  $L_{\beta}'$  (regular gel) phase, whereas patch domains are in the  $P_{\beta}'$  (rippled gel) phase. In contrast, Schmidt et al. reported that  $^2\text{H}$  NMR spectra of MLVs of DOPC/DPPE showed no evidence for the presence of  $P_{\beta}'$  phase [11]. The temperature values at which patch domains appeared in our CFM images of 40:60 mol% DOPC/DPPE GUVs (on cooling the sample) correlate well with the onset of  $l_d$ - $L_{\beta}'$  phase co-existence as determined by  $^2\text{H}$  NMR. Since our fluorescence labeling experiments indicated different domain partitioning behavior for Rh-DPPE and DiI $_{18}$  compared to that reported by Li and Cheng [6] (see Sections 3.2.1, 3.2.3 and 3.2.4), we will regard both the patch and fibril domains as gel phases without commenting on the molecular organization of the lipids within these domains. A systematic study validating the lever rule on GUVs of DOPC/DPPE mixtures, similar to that presented by Fidorra et al. [18] for GUVs of 1,2-dilauroyl-*sn*-glycero-3-phosphocholine (DLPC)/DPPE, could represent a useful starting point in resolving these discrepancies.

### 3.2. Fluorescent probe partitioning in GUVs of 40:60 mol% DOPC/DPPE

We selected six fluorescent lipid analogs commonly used in phase separation studies of model membranes (see supplementary Fig. S1), and determined their partitioning preference in the DOPC/DPPE mixture qualitatively, by visual inspection of the fluorescence intensity signal in separate detection channels. Fluorescence cross-talk was ruled out as described in Section 2.3; this was especially important when NBD-DPPE and DiI $_{18}$  were used together as fluorescent probes.

#### 3.2.1. Triple labeling with NBD-DPPE/DiI $_{18}$ /DiD

We first used a triple labeling approach with NBD-DPPE, DiI $_{18}$ , and DiD as fluorescent probes (each at 0.1 mol%). We selected these probes because of their observed partitioning preference in GUVs of ternary lipid mixtures [5]. NBD-DPPE was found to prefer the liquid-ordered ( $l_o$ ) phase in DOPC/DPPE/cholesterol ternary mixtures, thus we expected gel phase partitioning for this probe. We previously assigned no partitioning preference for DiI $_{18}$  when it was used

together with NBD-DPPE and DiD in triple labeling experiments, and DiD proved to have a strong preference for  $l_d$  phase, with the advantage of high excitation/emission wavelength.

The highest temperature examined for this sample was 35.4 °C, at which we observed quasi-circular patch domains on the surface of the GUVs, from which all three fluorescent probes were excluded. On gradually decreasing the temperature, fibril domains started to form on the vesicle surface at 24.7 °C; this was readily observable in larger GUVs with a diameter > 10  $\mu\text{m}$ . The fibril domains were observed to be more extended on the surface of GUVs when compared with the deuterated sample in Fig. 1F (not shown). On further cooling, the number of fibril domains increased considerably, and the fibrils

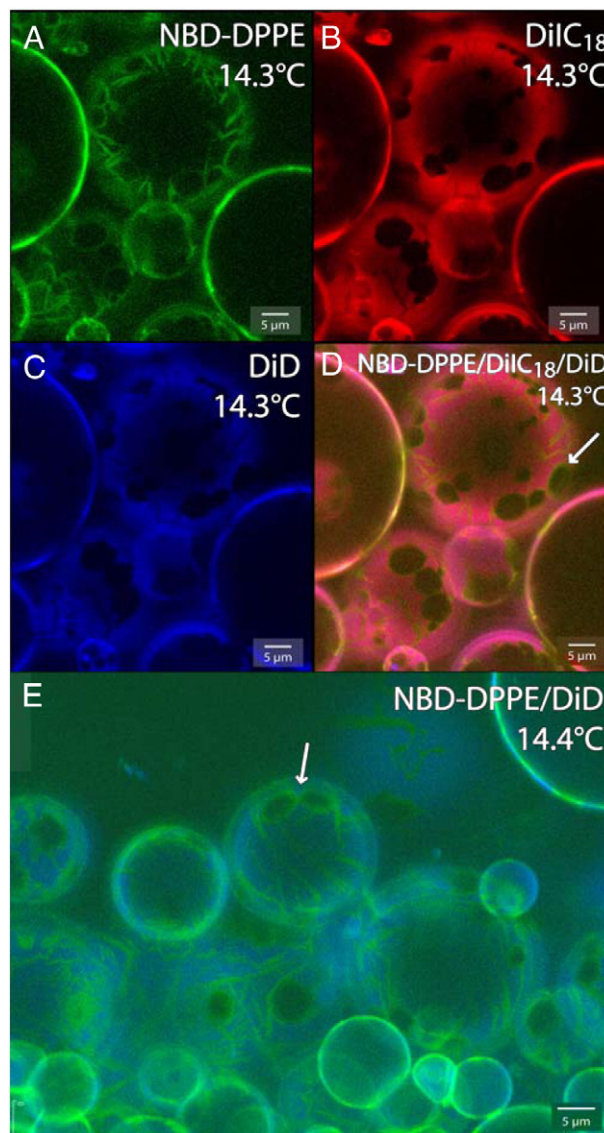


**Fig. 2.** Triple labeling in GUVs of DOPC/DPPE: NBD-DPPE/DiI $_{18}$ /DiD. CFM images of 40:60 mol% DOPC/DPPE GUVs at 14.3 °C (A–D) and at 14.4 °C (E) labeled with three probes simultaneously. (A) NBD-DPPE (green) partitions very strongly into the fibril domains; (B) DiI $_{18}$  (red) and (C) DiD (blue) are excluded from both patch and fibril domains. (D) is an overlay of the three fluorescence images. (E) is an overlay image of the acquired images in the NBD-DPPE (green) and DiD (blue) detection channels. Arrows indicate that fibril domains are wrapped around patch domains. Images in (A–D) were recorded after ~90 min and in (E) after ~160 min of temperature equilibration. No other domains in addition to patch and fibril were evident.

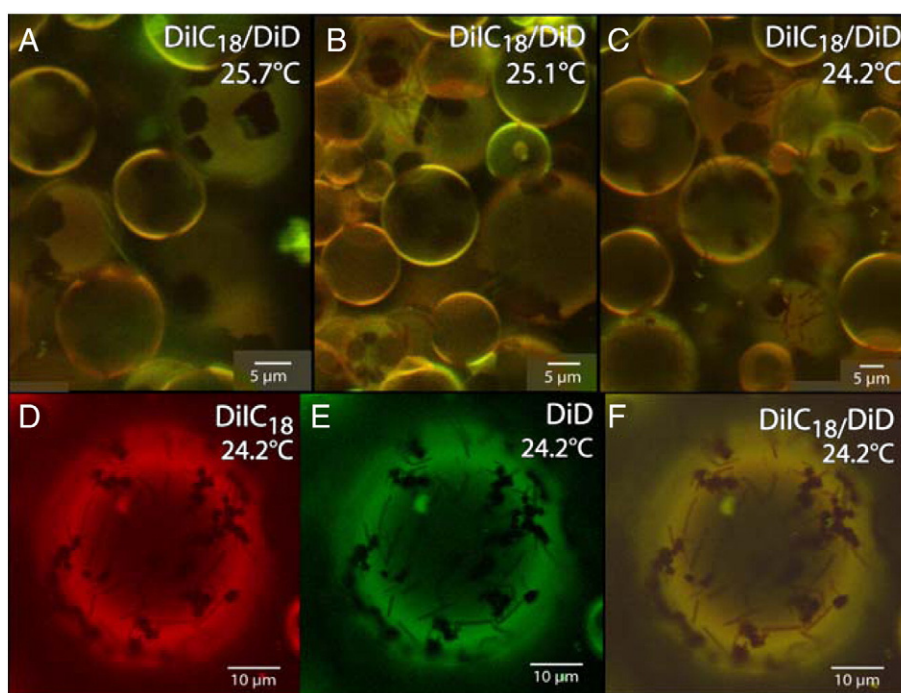


**Fig. 3.** Dual labeling in GUVs of DOPC/DPPC: DiIC<sub>18</sub>/DiD. CFM images of 40:60 mol% DOPC/DPPC GUVs co-labeled with DiIC<sub>18</sub> (red) and DiD (green). Detection and evolution of fibril domains is seen in the overlay images from the two separate detection channels in (A) at 25.7 °C, (B) at 25.1 °C, and (C) at 24.2 °C. A representative GUV at 24.2 °C is shown in (D) DiIC<sub>18</sub> (red), (E) DiD (green), and (F) an overlay of the two. Both probes are localized in the *l<sub>d</sub>* phase.

became somewhat wider. We identified the presence of fibril domains in virtually every GUV regardless of size, and in all regions of the Pt wires where lipid droplets were originally deposited. The partitioning preference of the three fluorescent probes when used simultaneously at 14.3 °C is presented in Fig. 2. NBD-DPPE (in green, Fig. 2A) was found exclusively in fibril domains, whereas DiIC<sub>18</sub> (in red, Fig. 2B) and DiD (in blue, Fig. 2C) were excluded from both fibril and patch domains. In the overlay image in Fig. 2D, patch domains on the surface of the GUVs remained dark, reflecting the exclusion of all three fluorescent probes from these domains. A closer examination of the overlay image revealed an increased amount of NBD-DPPE green fluorescence intensity around the edges of patch domains (indicated by the arrow in Fig. 2D). The fluorescence intensity images of NBD-DPPE represent a clear visualization of the interconnected, network-forming structure of fibril domains. In this CFM image, it is also readily observed that the fibril domains enclose the edges of the patch domains. This effect is not visible in either of the DiIC<sub>18</sub> or DiD fluorescence intensity images, where both the fibril and the patch domains remained dark on a bright background. More convincing evidence of this effect is presented in Fig. 2E. This image is an overlay of only NBD-DPPE (green) and DiD (blue) intensity images, while the excitation and emission of DiIC<sub>18</sub> was turned off. DiD is obviously excluded from the fibril domains labeled by the NBD-DPPE, and the localization of fibril domains around the edges of the patch domains is clearly visible. As a result, NBD-DPPE proved to be a very effective fluorescent probe in visualizing fibril domains in GUVs of DOPC/DPPC (Table 1). The relatively low temperature of ~14 °C was probed for this sample only, in order to check whether any other gel phases, such as the sub-gel phase (*L<sub>c</sub>'*), become visible. <sup>2</sup>H NMR measurements suggest that, in principle, in samples of 40:60 mol% undeuterated DOPC/DPPC, the *l<sub>d</sub>* phase is in equilibrium with the sub-gel phase. In other model membranes, the conversion from gel to sub-gel phase has proved to be very slow, from several hours to many days [11]. However, we did not detect any additional domains compared to those present at room temperature during a 4.5 h

observation period. The images in Fig. 2A–D were acquired ~90 min after the temperature reached equilibrium at 14.5 °C, whereas the image in Fig. 2E was acquired after ~160 min.

Interestingly, DiIC<sub>18</sub> preferred the *l<sub>d</sub>* phase in this binary lipid mixture (Table 1), as opposed to having no partitioning preference when used with the same fluorescent probes in ternary DOPC/DPPC/cholesterol mixtures. DiIC<sub>18</sub> was excluded from the fibril domains, in contrast to the previously reported preference of this probe for fibril domains in GUVs of DOPC/DPPC [6]. In other studies on GUVs of binary lipid mixtures, DiIC<sub>18</sub> was found to partition into either the fibril or *l<sub>d</sub>* domains depending on the lipid host system [4,17,19]. The inconsistencies in the observed partitioning behavior of DiIC<sub>18</sub> between our study and that of Li and Cheng [6] reinforce the importance of

**Table 1**  
Lipid domain partitioning preferences of various fluorescent probes in GUVs of DOPC/DPPC.

Fluorescent probe	Domain partitioning preference		
	Single labeling	Dual labeling	Triple labeling
TR-DPPE	<i>l<sub>d</sub></i>	<i>l<sub>d</sub></i>	<i>l<sub>d</sub></i>
DiIC <sub>18</sub>	–	<i>l<sub>d</sub></i>	<i>l<sub>d</sub></i>
DiD	–	<i>l<sub>d</sub></i>	<i>l<sub>d</sub></i>
Bodipy-PC	–	<i>l<sub>d</sub></i>	<i>l<sub>d</sub></i>
Rh-DPPE	<i>l<sub>d</sub></i> + ?fibril	<i>l<sub>d</sub></i> + ?fibril	<i>l<sub>d</sub></i> + ?fibril
NBD-DPPE	–	Fibril	Fibril

Notes:

1. All fluorescent probes were excluded from patch domains.
2. When Rh-DPPE was used in combination with other fluorescent probes, no fibril domains were detected in the temperature range examined.
3. ? Indicates that either the probe partitions equally between *l<sub>d</sub>* and fibril domains, or no fibril domains exist, or if they do exist they are smaller than the resolution of the confocal microscope.



subtle differences in the technical details of sample preparation and imaging protocols, such as generating GUVs on Pt wires vs. using ITO coverslips, and imaging the vesicles attached to the Pt wires vs. manipulating them after vesicle generation. For example, preparing GUVs on Pt wires and imaging the sample without any further vesicle manipulation might lead to a different surface tension than the ITO method.

### 3.2.2. Dual labeling with DiIC<sub>18</sub>/DiD

The temperature-dependent experiments started at 39.7 °C, where very small patch domains were observed on the surface of most GUVs. Both fluorescent probes partitioned away from these domains. At 31.4 °C, the temperature controller was turned off, and the temperature of the sample was allowed to gradually equilibrate to room temperature (24.2 °C). During this time period several images were acquired. Images of DiIC<sub>18</sub> (red) and DiD (green) acquired in separate detection channels are presented in Fig. 3A–C, as overlays. At 25.7 °C, the formation of a small number of fibril domains on the surface of some GUVs was observed (lower left corner in Fig. 3A). However, on further cooling to 25.1 °C, the number of these domains increased considerably (Fig. 3B), and it can be seen that both fluorescent probes are excluded from patch and fibril domains. Over the course of 10 min (from the acquisition of the image in Fig. 3B) the temperature reached 24.2 °C, and the formation of additional fibril domains became obvious during this time (Fig. 3C–F). Although the temperature change was <1 °C, the number of fibril domains increased considerably, which we attribute not only to the temperature change, but also to the slower process of domain equilibration mentioned above. A close-up view of a single GUV is presented in Fig. 3, showing images from the two separate detection channels (Fig. 3D and E) and an overlay (Fig. 3F). Comparing images acquired at 24.2 °C (Fig. 3F) and 14 °C (Fig. 2D), we conclude that the fibril domains are only modestly thicker at lower temperatures. Upon heating the sample the fibril domains melted into the l<sub>d</sub> phase at ~30 °C (not shown). Similar results were also reported for GUVs of 20:80 mol% DOPC/DPPC, where the fibril domains vanished upon heating to ~40 °C and reappeared at ~31 °C when cooling the sample [6].

### 3.2.3. Triple labeling with Bodipy-PC/Rh-DPPE/DiD

Another interesting combination of probes with a surprising outcome was Bodipy-PC, Rh-DPPE, and DiD. The total amount of fluorescent probe in this sample was 0.15 mol%, with each probe at 0.05 mol%. In previous studies it was found that Rh-DPPE segregated into fibril domains and Bodipy-PC was excluded from fibril domains, in GUVs of DOPC/DPPC [6] and other binary lipid mixtures [4,17,20–23]. Contrary to these findings, our findings on the partitioning preference of these three labels when used together were very different, as presented in Fig. 4. Surprisingly, no fibril domains were visible in the 33.0–23.1 °C temperature range, even though the sample was equilibrated at ~23 °C for ~40 min. However, all three fluorescent probes, Bodipy-PC (in green, Fig. 4A), Rh-DPPE (in red, Fig. 4B), and DiD (in blue, Fig. 4C) were excluded from patch domains. An overlay of the fluorescence intensities of all three probes is presented in Fig. 4D. The absence of visible fibril domains in these images is obvious; if very thin fibril domains exist, they are certainly below the resolution of the confocal microscope. Therefore, these three labels, when used together, present a different view of the phase behavior of DOPC/DPPC GUVs. In interpreting these images, we conclude that either no fibril domains exist in GUVs labeled by these three probes, or all three probes partition with an equal ratio into l<sub>d</sub> and fibril domains. The latter explanation seems unrealistic considering the results of further investigations below. To characterize which one of the three lipid probes was responsible for the absence of fibril domains, we examined the same binary mixture labeled only

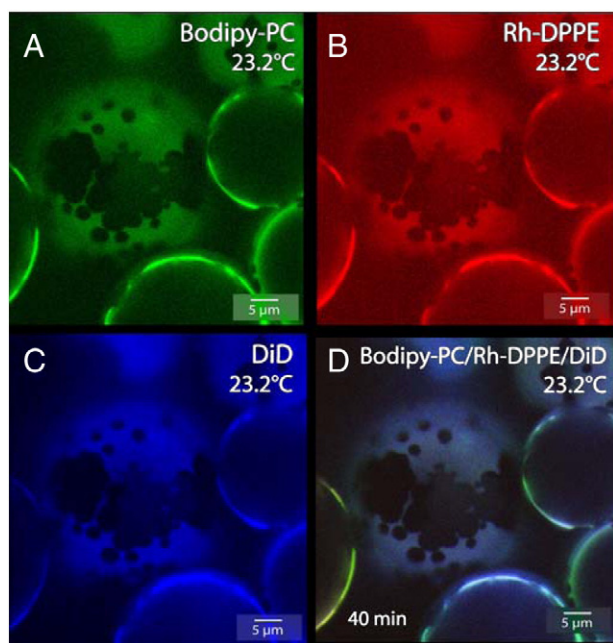


**Fig. 4.** Triple labeling in GUVs of DOPC/DPPC: Bodipy-PC/Rh-DPPE/DiD. CFM images of 40:60 mol% DOPC/DPPC GUVs labeled with three probes simultaneously, which exhibit no fibril domains after 40 min sample equilibration at 23.2 °C. (A) Bodipy-PC (green), (B) Rh-DPPE (red), (C) DiD (blue), and (D) overlay of the three images. All three labels partition into the l<sub>d</sub> phase.

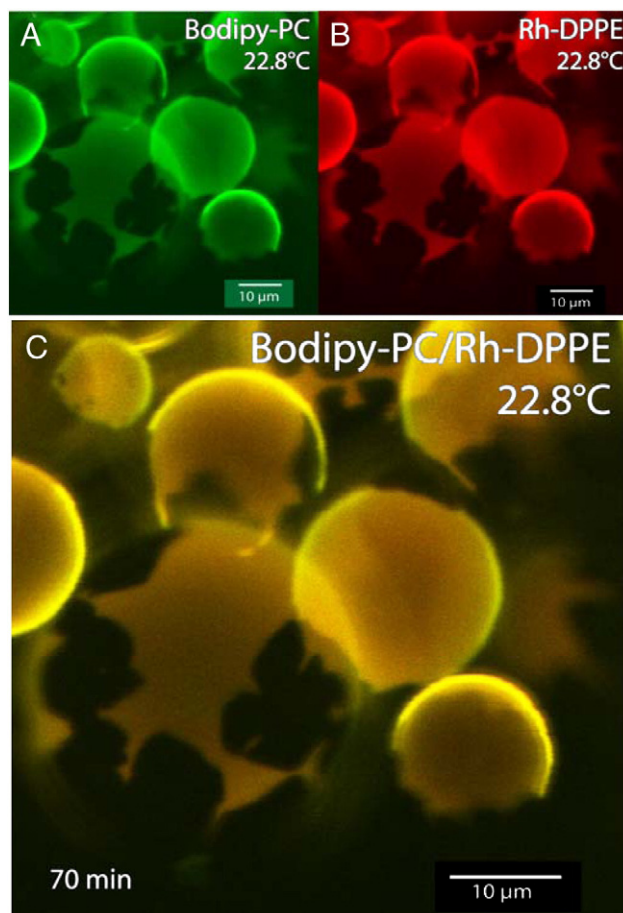


**Fig. 5.** Dual labeling in GUVs of DOPC/DPPC: Bodipy-PC/Rh-DPPE. CFM images of 40:60 mol% DOPC/DPPC GUVs co-labeled with (A) Bodipy-PC (green) and (B) Rh-DPPE (red) at 22.8 °C. No fibril domains are visible even after temperature equilibration for 70 min. Both labels are excluded from patch domains.

with Rh-DPPE, then dual labeled with Bodipy-PC/Rh-DPPE, and Bodipy-PC/DiI<sub>C18</sub> (see below).

### 3.2.4. Labeling with Rh-DPPE and Bodipy-PC/Rh-DPPE

In GUVs of 40:60 mol% DOPC/DPPC, the presence of Rh-DPPE, either as a single label or when used as a dual label with Bodipy-PC, made it impossible to detect fibril domains in the 41–22 °C temperature range. In Fig. 5, images acquired at 22.8 °C from the dual labeling experiment are shown (Bodipy-PC in green, Fig. 5A; Rh-DPPE in red, Fig. 5B) and an overlay of the fluorescence intensity images of the two probes is presented in Fig. 5C. Both probes partitioned away from patch domains, which appeared dark in the overlay image. Similar images to that shown in Fig. 5B were also recorded for the Rh-DPPE single labeling experiment (not shown). Fibril domain formation is affected by the cooling rate, since it takes a short time (~5 min) for them to evolve and reach equilibrium. However, we observed that fibril domains formed regardless of the cooling rate (0.2–2 °C/min). We typically varied the temperature in small 2 °C steps (corresponding to a cooling rate of 1–2 °C/min), and when the sample was allowed to cool to room temperature immediately after vesicle generation (at ~60 °C) the estimated average cooling rate was ~0.5 °C/min. However, Bernchou et al. [14] concluded that the density of individual patch domains observed in supported bilayers was directly proportional to the cooling rate within the range 0.15–3.50 °C/min. In their studies they used continuous cooling from 40–25 °C, whereas in the present study the temperature was kept constant for the period of image acquisition after each 2 °C step-wise change. We also observed no difference in domain size or appearance when the sample was cooled in 2 °C steps compared to being simply allowed to equilibrate to room temperature.

### 3.2.5. Dual labeling with Bodipy-PC/DiI<sub>C18</sub>

As the sample was slowly cooled from 45.8 °C to room temperature in 2 °C steps, we observed a considerable increase in size of the patch domains between 38 and 34 °C. Representative GUVs at 33.5 °C are shown in Fig. 6A–D, where the fluorescence intensities of Bodipy-PC and DiI<sub>C18</sub> appear as red and green, respectively. Both probes were excluded from the patch domains, and no fibril domains were detectable at this temperature. The sample was then equilibrated at 24.7 °C for ~1 h, and new images were acquired (Fig. 6E–F). Fibril domains were detected in virtually all GUVs, and both labels

showed the same partitioning behavior, since the fluorescence intensities of Bodipy-PC (red, Fig. 6D) and DiI<sub>C18</sub> (green, Fig. 6E) were identical. No fluorescence signal was detected in the patch and fibril domains; thus, in the overlay image (Fig. 6F) both types of domains appear dark on the GUV surface.

## 4. Conclusions

In previous work, we characterized the phase partitioning behavior of several commonly used fluorescent probes in ternary mixtures of DOPC/DPPC/cholesterol, which display co-existence of *l<sub>d</sub>* and *l<sub>o</sub>* phases. In the present study, this approach was extended to GUVs of DOPC/DPPC, which exhibit *l<sub>d</sub>*-gel phase co-existence, with the goal of determining whether the various fluorescent probes report on the same phase behavior. This binary mixture has been reported to display interesting phase behavior, with two novel gel phases, patch and fibril, observed by CFM [6]. In our study, we made use of the recently published binary phase diagram determined by <sup>2</sup>H NMR for the DOPC/DPPC-d<sub>62</sub> lipid system [11]. The combined use of CFM and <sup>2</sup>H NMR as complementary techniques provides a powerful approach for systematic investigation and interpretation of lipid phase behavior. Using TR-DPPE, which has proved to be a reliable probe of the *l<sub>d</sub>* phase [5,9], we found that the onset temperature of the *l<sub>d</sub>*-gel phase transition in GUVs qualitatively resembles the values determined by <sup>2</sup>H NMR for the same mixture, particularly when DPPC-d<sub>62</sub> was used as one component.

Both patch and fibril domains were detected on the surface of GUVs of 40:60 mol% DOPC/DPPC depending on the temperature and the fluorescent probe employed. Table 1 summarizes the partitioning preference for *l<sub>d</sub>*, patch and fibril domains of the various probes in single/dual/triple situations. All the fluorescent probes used in this study were excluded from the patch domains. We found that NBD-DPPE labeled the fibril domains; indeed, partitioning of the probe into these domains was so strong that virtually no fluorescence intensity was detected in the *l<sub>d</sub>* domains. The ability of NBD-DPPE to insert itself in tightly packed regions in the membrane is probably due to its small fluorophore and saturated acyl chains. This may explain why it was found almost exclusively in fibril domains on the surface of GUVs in this study, and in *l<sub>o</sub>* domains in ternary mixtures [5]. However, even the presence of the small NBD fluorophore did not allow NBD-DPPE to partition into the patch domains.

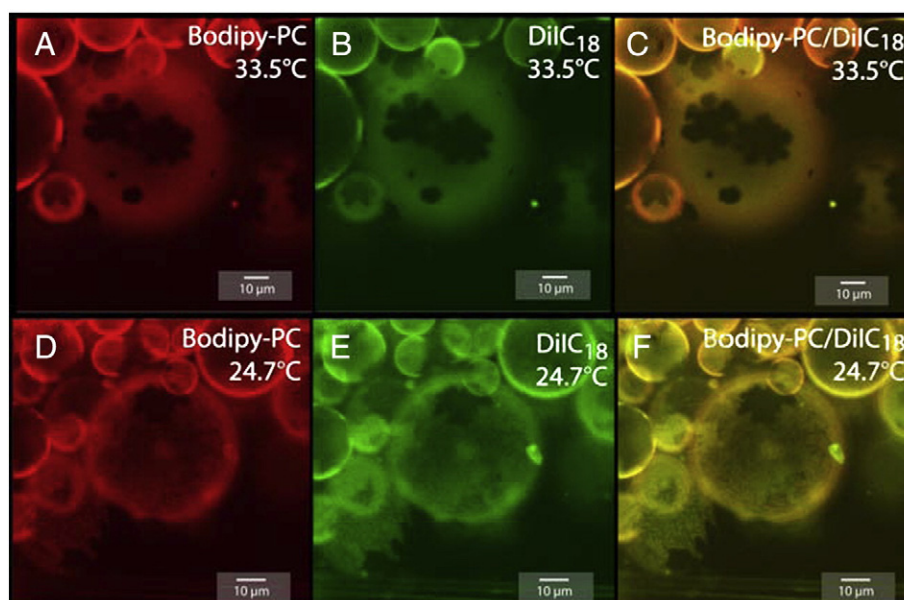


**Fig. 6.** Dual labeling in GUVs of DOPC/DPPC: Bodipy-PC/DiI<sub>C18</sub>. CFM images of 40:60 mol% DOPC/DPPC GUVs co-labeled with (A and D) Bodipy-PC (red) and (B and E) DiI<sub>C18</sub> (green) at 33.5 °C (A–C) and at 24.7 °C (D–F). Fibril domains are present at 24.7 °C, and both probes were excluded from fibril and patch domains.



There is currently little information available on the molecular nature of the fibril and patch domains. If the patch domains indeed represent rippled gel phase ( $P_{\beta}'$ ), clearly the packing properties of this phase make it difficult for any of the fluorescent probes, even NBD-DPPE, to partition into it.

All the fluorescent probes used in the present study are headgroup-labeled lipid analogs except Bodipy-PC, where the fluorophore is attached to one of the acyl chains. It is interesting to note that even though TR-DPPE and Rh-DPPE have very similar structures, and both partition into  $I_d$  domains, we found that they reported different phase behavior in GUVs of DOPC/DPPC.

Previous characterization by Li and Cheng of the different gel phases present in GUVs of DOPC/DPPC mixtures was not exhaustive, and, for the most part, used only two fluorescent probes, Rh-DPPE and Bodipy-PC [6]. However, they present valuable information on how different parameters such as surface tension might affect the observation of different domains on the surface of GUVs. We found major inconsistencies in the partitioning behavior of Rh-DPPE and DiI<sub>C18</sub> when comparing our results with those they reported for the same system [6]. Li and Cheng observed fibril domains labeled by Rh-DPPE in GUVs of 40:60 mol% DOPC/DPPC, whereas our results indicate no preferential partitioning of Rh-DPPE into these domains using the same lipid mixture at the same temperature. It is possible that sample preparation differences are responsible for these inconsistencies (differences between our method and theirs are highlighted in Section 2.2). Overall, this raises concern about the universal validity of the results of phase behavior studies when limited numbers of fluorescent reporters are explored. Aggregated results, such as partial phase diagrams, constructed from the results of different experimental techniques may represent a valuable aid in elucidating artifact-free phase behavior.

The presence of fluorescent probe Rh-DPPE resulted in no fibril domains being detected, and this effect was extended to other fluorescent probes when used in dual or triple labeling with Rh-DPPE. All the fluorescent probes used in this study showed consistent partitioning behavior in GUVs of 40:60 mol% DOPC/DPPC in the absence of Rh-DPPE. However, when Rh-DPPE was present as one of the labels, either the partitioning preference of the other labels was perturbed, or it influenced the phase behavior of the whole system. Our results reaffirm the importance of examining the partitioning behavior of fluorescent probes in a given model membrane system before drawing firm conclusions about either the phase preference of fluorescent probes or the phase behavior of the system.

Overall, the multiple labeling approach used in the present study proved to be a valuable tool for characterizing various fluorescent probes in GUVs, and in detecting subtle differences in the phase behavior of phospholipids in the presence of these lipid analogs. In particular, the triple labeling approach revealed how Rh-DPPE may report different phase behavior in GUVs of DOPC/DPPC, and how it may potentially alter the partitioning behavior of other fluorescent probes when used simultaneously, even at very low (0.05 mol%) labeling levels. The partitioning of a particular fluorescent probe into a membrane domain appears to depend not only on its phase state, but also on the chemical nature and local environment within that domain, which in turn depends on lipid composition. Thus, phase partitioning preferences may be valid only for the specific model system being investigated. Our experiments on binary and ternary mixtures of DOPC/DPPC and DOPC/DPPC/cholesterol [5,9] constitute a firm basis for systematic characterization of commonly used fluorescent probes in membrane phase separation studies.

Supplementary materials related to this article can be found online at doi:10.1016/j.bbamem.2011.09.006.

## Acknowledgments

We are grateful for the technical assistance of Michaela Struder-Kypke and Joseph Chu. This work was supported by grants to FJS and JHD from the Natural Sciences and Engineering Research Council of Canada, the Canada Foundation for Innovation and the Ontario Research Fund.

## References

- [1] R. Lindner, H.Y. Naim, Domains in biological membranes, *Exp. Cell. Res.* 315 (2009) 2871–2878.
- [2] D. Lingwood, K. Simons, Lipid rafts as a membrane-organizing principle, *Science* 327 (2010) 46–50.
- [3] K. Simons, E. Ikonen, Functional rafts in cell membranes, *Nature* 387 (1997) 569–572.
- [4] L.A. Bagatolli, To see or not to see: lateral organization of biological membranes and fluorescence microscopy, *Biochim. Biophys. Acta* 1758 (2006) 1541–1556.
- [5] J. Juhasz, J.H. Davis, F.J. Sharom, Fluorescent probe partitioning in giant unilamellar vesicles of 'lipid raft' mixtures, *Biochem. J.* 430 (2010) 415–423.
- [6] L. Li, J.X. Cheng, Coexisting stripe- and patch-shaped domains in giant unilamellar vesicles, *Biochemistry* 45 (2006) 11819–11826.
- [7] M.I. Angelova, D.S. Dimitrov, Liposome electroformation, *Faraday Discuss. Chem. Soc.* 81 (1986) 303–311.
- [8] D.S. Dimitrov, M.I. Angelova, Lipid swelling and liposome formation mediated by electric fields, *Bioelectrochem. Bioenergetics* 19 (1988) 323–336.
- [9] J. Juhasz, F.J. Sharom, J.H. Davis, Quantitative characterization of coexisting phases in DOPC/DPPC/cholesterol mixtures: comparing confocal fluorescence microscopy and deuterium nuclear magnetic resonance, *Biochim. Biophys. Acta* 1788 (2009) 2541–2552.
- [10] S.L. Veatch, S.L. Keller, Organization in lipid membranes containing cholesterol, *Phys. Rev. Lett.* 89 (2002) 268101.
- [11] M.L. Schmidt, L. Ziani, M. Boudreau, J.H. Davis, Phase equilibria in DOPC/DPPC: Conversion from gel to subgel in two component mixtures, *J. Chem. Phys.* 131 (2009) 175103.
- [12] M.E. Beattie, S.L. Veatch, B.L. Stottrup, S.L. Keller, Sterol structure determines miscibility versus melting transitions in lipid vesicles, *Biophys. J.* 89 (2005) 1760–1768.
- [13] R. Elliott, K. Katsov, M. Schick, I. Szleifer, Phase separation of saturated and mono-unsaturated lipids as determined from a microscopic model, *J. Chem. Phys.* 122 (2005) 044904.
- [14] U. Bernchou, J.H. Ipsen, A.C. Simonsen, Growth of solid domains in model membranes: quantitative image analysis reveals a strong correlation between domain shape and spatial position, *J. Phys. Chem. B* 113 (2009) 7170–7177.
- [15] H. Bouvrais, T. Pott, L.A. Bagatolli, J.H. Ipsen, P. Meleard, Impact of membrane-anchored fluorescent probes on the mechanical properties of lipid bilayers, *Biochim. Biophys. Acta* 1798 (2010) 1333–1337.
- [16] N.F. Morales-Pennington, J. Wu, E.R. Farkas, S.L. Goh, T.M. Konyakhina, J.Y. Zheng, W.W. Webb, G.W. Feigenson, GUV preparation and imaging: minimizing artifacts, *Biochim. Biophys. Acta* 1798 (2010) 1324–1332.
- [17] P.A. Beales, V.D. Gordon, Z. Zhao, S.U. Egelhaaf, W.C.K. Poon, Solid-like domains in fluid membranes, *J. Phys. Condens. Matter* 17 (2005) S3341–S3346.
- [18] M. Fidorra, A. Garcia, J.H. Ipsen, S. Hartel, L.A. Bagatolli, Lipid domains in giant unilamellar vesicles and their correspondence with equilibrium thermodynamic phases: a quantitative fluorescence microscopy imaging approach, *Biochim. Biophys. Acta* 1788 (2009) 2142–2149.
- [19] J.B. De la Serna, J. Perez-Gil, A.C. Simonsen, L.A. Bagatolli, Cholesterol rules – Direct observation of the coexistence of two fluid phases in native pulmonary surfactant membranes at physiological temperatures, *J. Biol. Chem.* 279 (2004) 40715–40722.
- [20] L.A. Bagatolli, E. Gratton, Two photon fluorescence microscopy of coexisting lipid domains in giant unilamellar vesicles of binary phospholipid mixtures, *Biophys. J.* 78 (2000) 290–305.
- [21] L.A. Bagatolli, Thermotropic behavior of lipid mixtures studied at the level of single vesicles: giant unilamellar vesicles and two-photon excitation fluorescence microscopy, *Methods Enzymol.* 367 (2003) 233–253.
- [22] G.W. Feigenson, J.T. Buboltz, Ternary phase diagram of dipalmitoyl-PC/dilauroyl-PC/cholesterol: nanoscopic domain formation driven by cholesterol, *Biophys. J.* 80 (2001) 2775–2788.
- [23] J. Korlach, P. Schwille, W.W. Webb, G.W. Feigenson, Characterization of lipid bilayer phases by confocal microscopy and fluorescence correlation spectroscopy, *Proc. Natl. Acad. Sci. U. S. A.* 96 (1999) 8461–8466.